Electronic Supporting Information for

Mechano-responsive luminescent emissions of an organic molecular crystal: Effects of aromatic stacking interactions and solid state packing

Kakali Devi, Rupam J. Sarma*
Department of Chemistry, Gauhati University, Guwahati 781014 Assam, India
Tel: +9198641 28514; Fax: +913612570535; E-mail: rjs@gauhati.ac.in

Table of Contents

1. General experimental techniques.

All chemicals were commercially available from Sigma-Aldrich and/or Merck and used as received. Solvents for spectroscopic experiments were distilled under nitrogen atmosphere before use. All ^{1}H and ^{13}C NMR were measured on a 300 MHz Bruker spectrometer, and reported in δ/ppm. The absorption spectra were recorded on a Shimadzu UV-vis spectrophotometer (Model UV-1800), and fluorescence spectra were recorded using a Hitachi F2500 fluorimeter. The FTIR measurements were performed on a Bruker ALPHA II spectrometer, equipped with Multireflection-ATR module with horizontal ZnSe crystal. The TGA measurements were performed on a Mettler-Toledo TGA (STARe) equipment, equipped with silica/platinum crucibles. The single crystal X-ray Diffraction data were collected on a Bruker SMART APEX II CCD diffractometer equipped with a graphite monochromator and a Mo-K_α fine-focus sealed tube (λ = 0.71073 Å). Data integration was done using SAINT. Intensities for absorption were corrected using SADABS. Structure solution and refinement were carried out using Bruker SHELXTL. The Powder X-ray Diffraction (PXRD) measurements were performed on a Rigaku Ultima IV X-ray powder diffractometer operating a Cu-K_α X-ray source, equipped with a Ni filter to suppress K_β emission and a D/teX Ultra high-speed position sensitive detector, and measurements were performed at room temperature, with a scan range $2\theta = 5–50°$, step size of 0.02°, and scan rate of 2° min^{-1}.

2. Synthetic Procedures

Synthesis of 2-NOH-S: To a stirred solution of semicarbazide hydrochloride (**2**, 1.0 mmol) and sodium acetate (1 mmol) in H_2O (2 ml) was added a solution of the 2-hydroxynaphthaldehyde (**1**, 1 mmol) in MeOH (2 ml). After being stirred at room temperature for 10 min, the solvent was evaporated under reduced pressure. The solid residue was rinsed with chloroform and recrystallised from aqueous methanol.

^{1}H NMR (300 MHz, DMSO-d_6) δ_H = 11.24 (1H, s, -OH), 10.27(1H, s, urea NH), 8.85 (1H, s, aldimine-CH), 8.38 (1H, d, *J = 8.8 Hz*, aromatic CH), 7.83 (1H, d, *J = 8.8 Hz*, aromatic CH), 7.54 (2H, d, *J = 7.2 Hz*, aromatic CH), 7.36 (1H, t, *J = 7.2 Hz*, aromatic CH), 7.17 (1H, d, *J= 8.8 Hz*, aromatic CH), 6.41 (1H, t, aromatic CH); ^{13}C NMR (300 MHz, DMSO) δ_H= 155.78, 139.81, 131.43, 131.17, 128.61, 127.85, 127.47, 123.25, 121.99, 118.24, 109.64 ppm; ES-MS: m/z 230.06 calc. for (M+H$^+$)

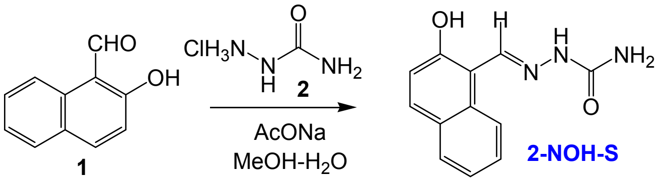

Crystallization of C-M and C-T

A known amount of the compound, **2-NOH-S**, was dissolved in a suitable solvent and the clear solution kept for crystallization at room temperature. In certain cases, the sample could be dissolved in the corresponding solvent, upon gentle heating at 60°C. The clear solution was kept at room temperature for crystallization.

Unless otherwise stated, the evaporation of solvent(s) was controlled by keeping the sample solutions in closed glass vial(s).

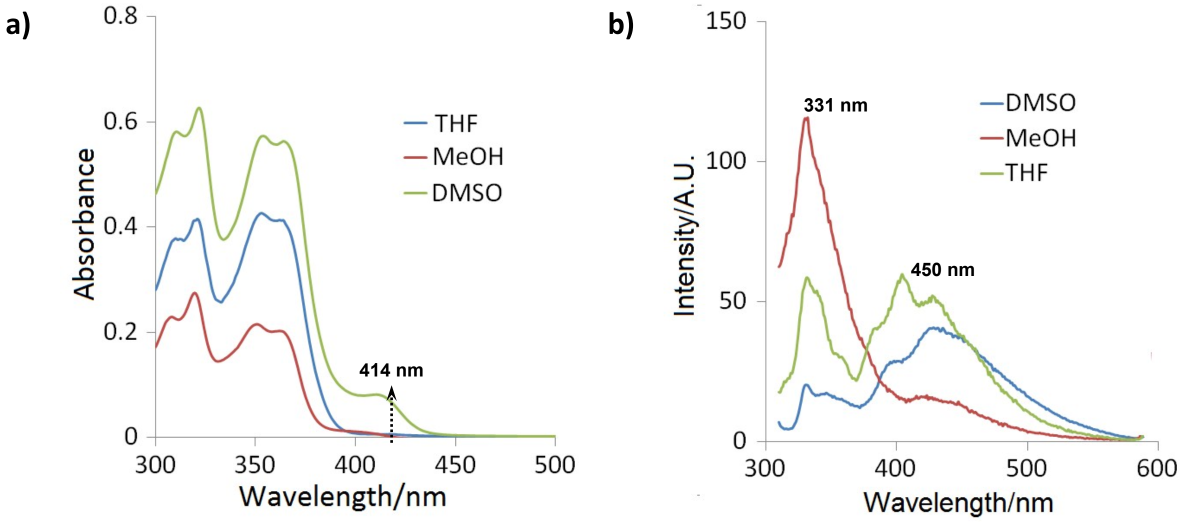

Figure S1: (a) UV-visible and (b) fluorescence spectra of **2NOH-S** (conc. 0.9 μM) in different solvents.

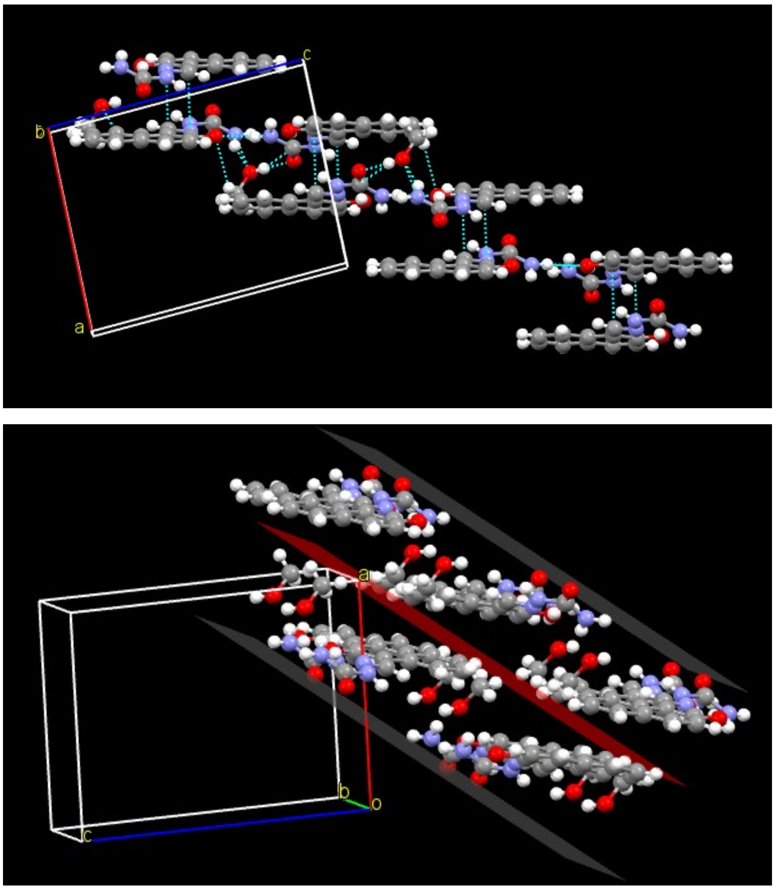

Figure S2: Packing diagram of **C-M** showing the intermolecular interactions between the **2-NOH-S** molecules in the lattice

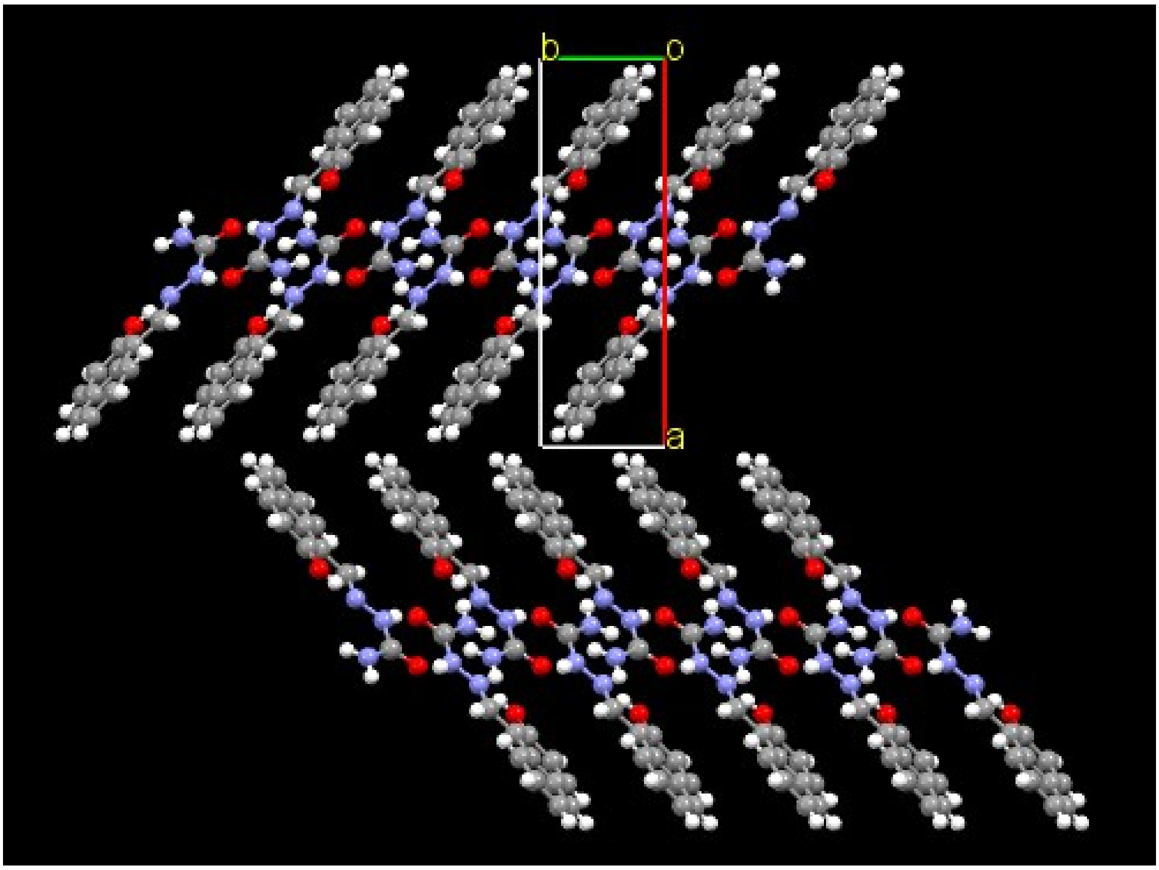

Figure S3: Packing diagram of **C-T** showing the intermolecular interactions between the **2-NOH-S** molecules in the lattice, showing the herringbone arrangements.

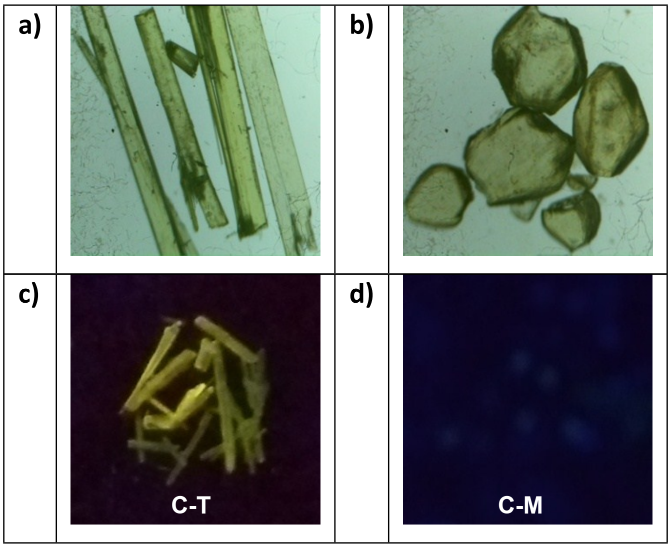

Figure S4. Images of needle-like and block shaped crystals of **C-T** and **C-M** respectively (a,b) under 10x magnification, and (c,d) when illuminated with 365 nm UV-light.

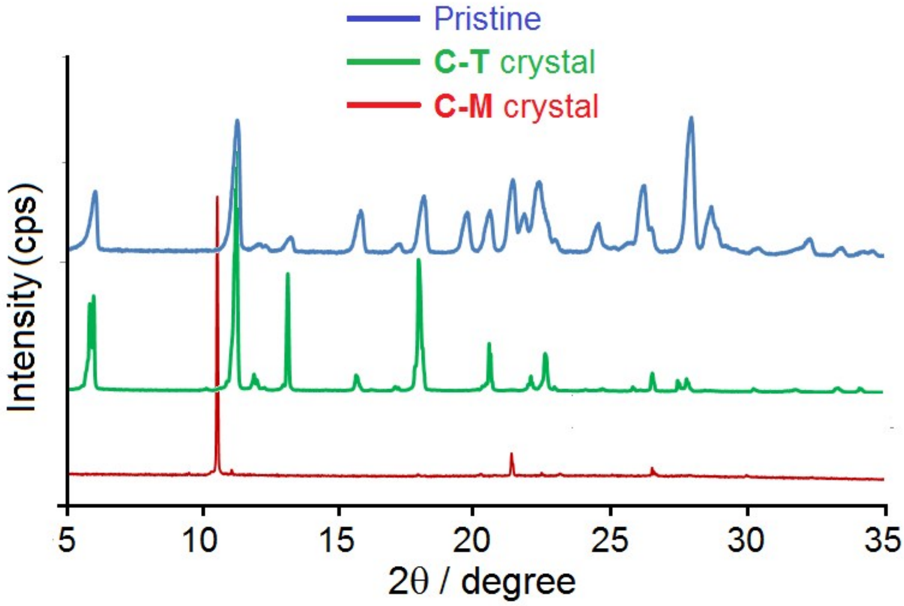

Figure S5: Powder XRD patterns of **C-M** and **C-T**, as compared to the pristine sample of **2-NOH-S**

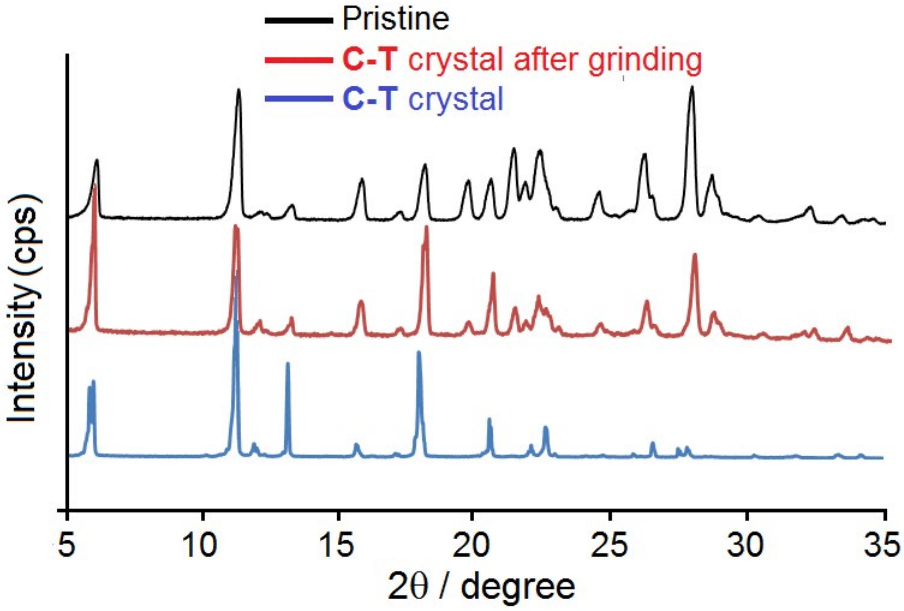

Figure S6: Changes in the powder XRD patterns of **C-T**, before and after grinding, as compared to the pristine sample of **2-NOH-S**

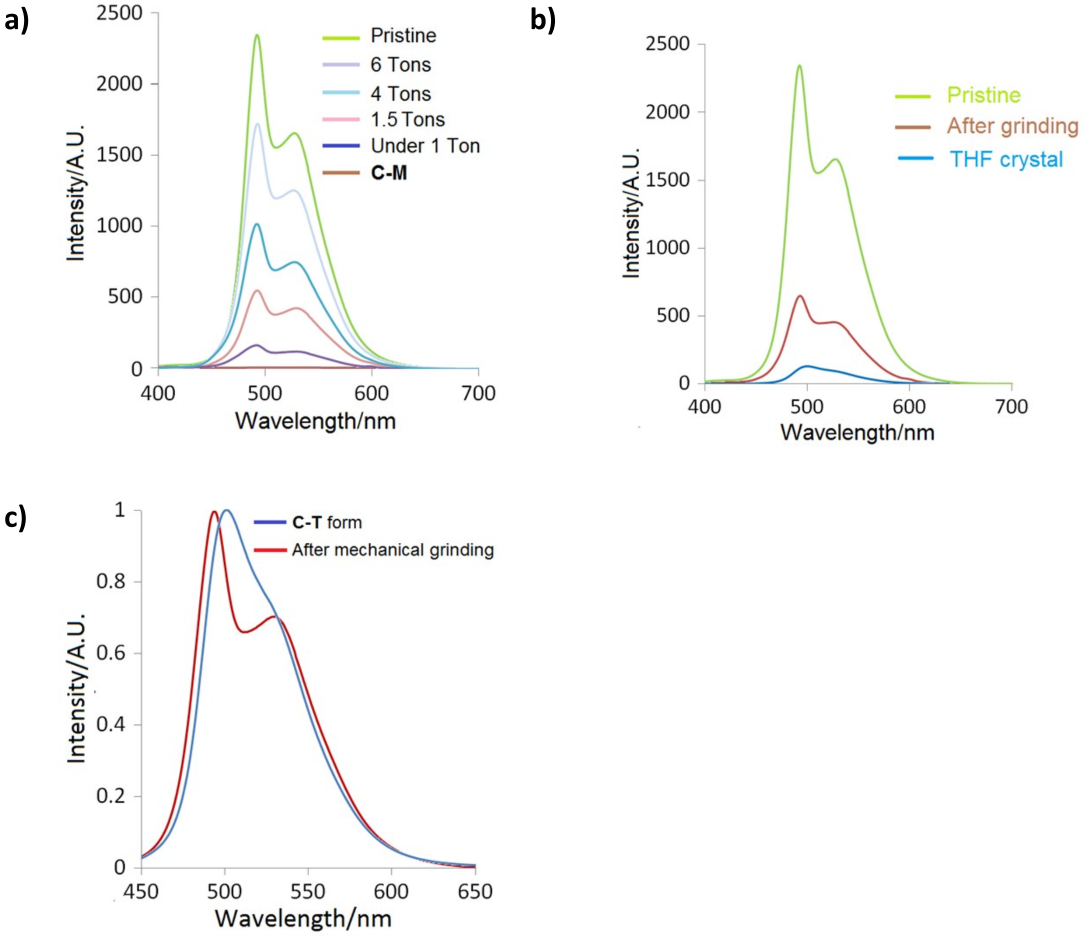

Figure S7: Effect of applied mechanical pressure on the solid state fluorescence spectra of (a) **C-M**, (b) **C-T** in comparison to pristine **2-NOH-S** sample

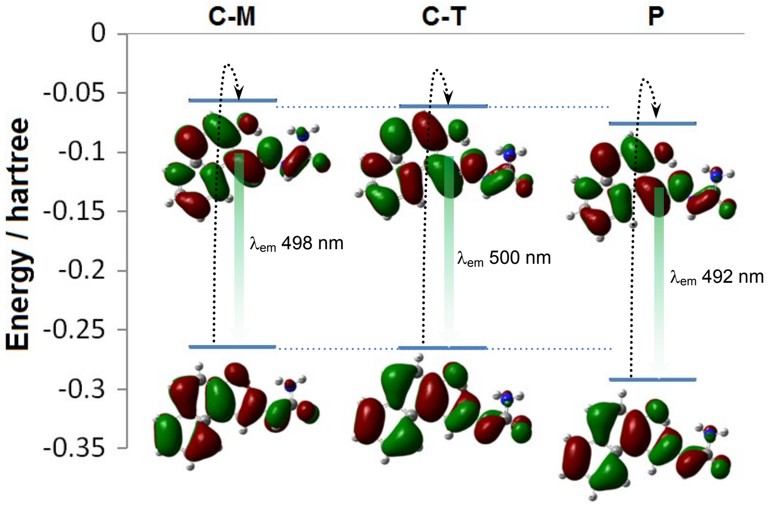

Figure S8: Calculated HOMO-LUMO energies for the **C-M** and **C-T** forms (from the crystal geometries), as compared to the optimized structure for **2-NOH-S** along with the corresponding emission maxima. The calculations were performed using Density Functional Theory (DFT) at B3LYP/6-31G(d,p) level of theory.

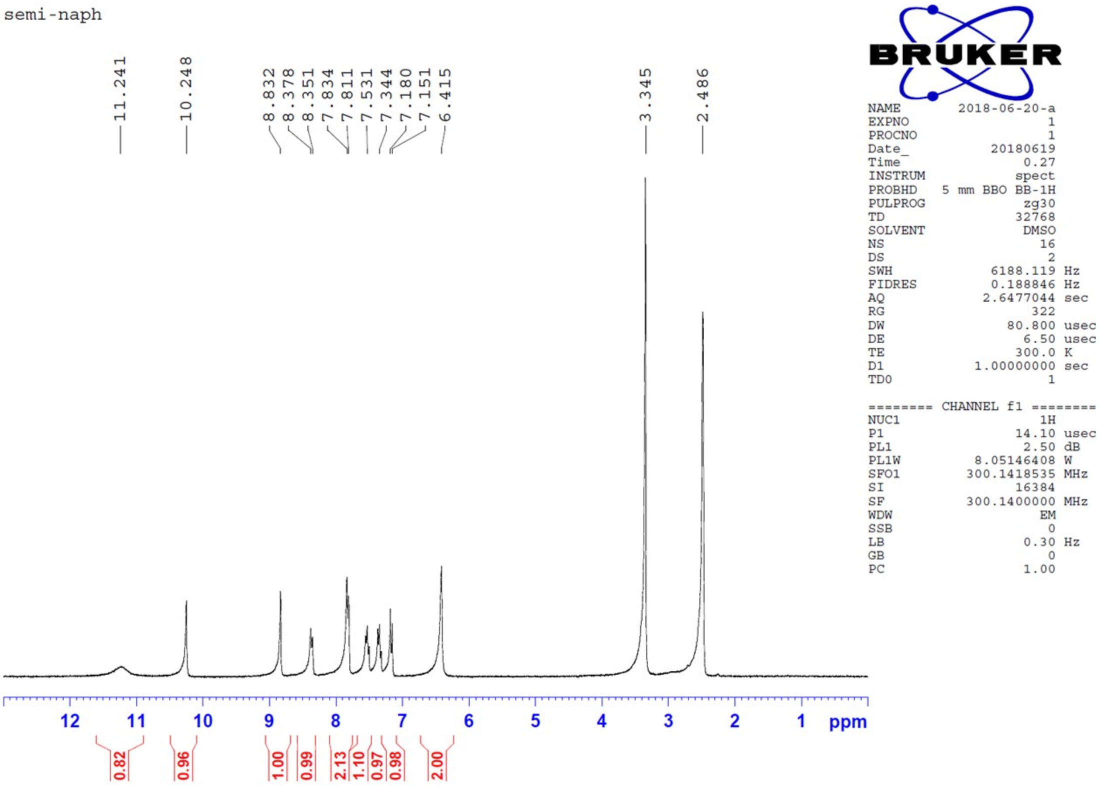

```
NAME        2018-06-20-a
EXPNO                  1
PROCNO                 1
Date_           20180619
Time                0.27
INSTRUM            spect
PROBHD   5 mm BBO BB-1H
PULPROG             zg30
TD                 32768
SOLVENT             DMSO
NS                    16
DS                     2
SWH             6188.119 Hz
FIDRES          0.188846 Hz
AQ             2.6477044 sec
RG                   322
DW                80.800 usec
DE                  6.50 usec
TE                 300.0 K
D1            1.00000000 sec
TD0                    1

======== CHANNEL f1 ========
NUC1                  1H
P1                 14.10 usec
PL1                 2.50 dB
PL1W          8.05146408 W
SFO1         300.1418535 MHz
SI                 16384
SF           300.1400000 MHz
WDW                   EM
SSB                    0
LB                  0.30 Hz
GB                     0
PC                  1.00
```

Figure S9: ^{1}H NMR spectra of **2-NOH-S** in DMSO-d$_6$

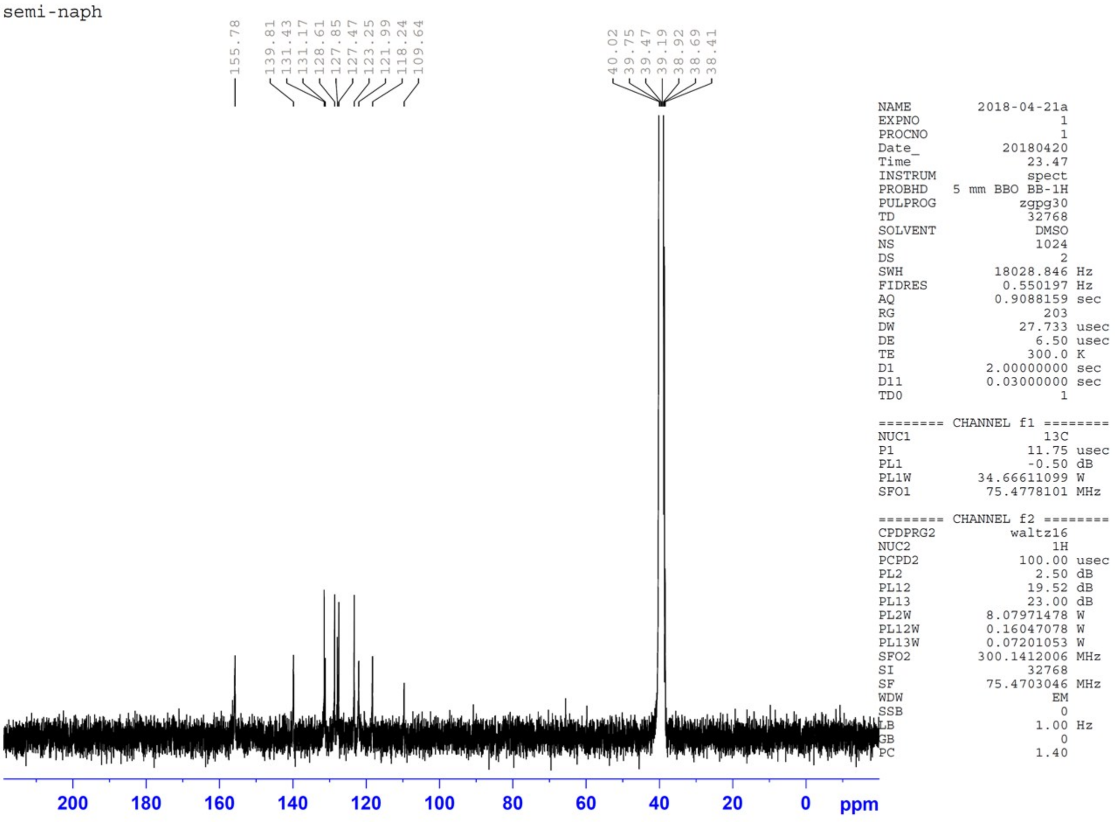

```
NAME        2018-04-21a
EXPNO                 1
PROCNO                1
Date_          20180420
Time              23.47
INSTRUM           spect
PROBHD   5 mm BBO BB-1H
PULPROG         zgpg30
TD                32768
SOLVENT            DMSO
NS                 1024
DS                    2
SWH           18028.846 Hz
FIDRES         0.550197 Hz
AQ            0.9088159 sec
RG                  203
DW               27.733 usec
DE                 6.50 usec
TE                300.0 K
D1           2.00000000 sec
D11          0.03000000 sec
TD0                   1

======== CHANNEL f1 ========
NUC1                13C
P1                11.75 usec
PL1               -0.50 dB
PL1W        34.66611099 W
SFO1         75.4778101 MHz

======== CHANNEL f2 ========
CPDPRG2         waltz16
NUC2                 1H
PCPD2            100.00 usec
PL2                2.50 dB
PL12              19.52 dB
PL13              23.00 dB
PL2W         8.07971478 W
PL12W        0.16047078 W
PL13W        0.07201053 W
SFO2        300.1412006 MHz
SI                32768
SF           75.4703046 MHz
WDW                  EM
SSB                   0
LB                 1.00 Hz
GB                    0
PC                 1.40
```

Figure S10: ^{13}C NMR spectra of **2-NOH-S** in DMSO-d$_6$

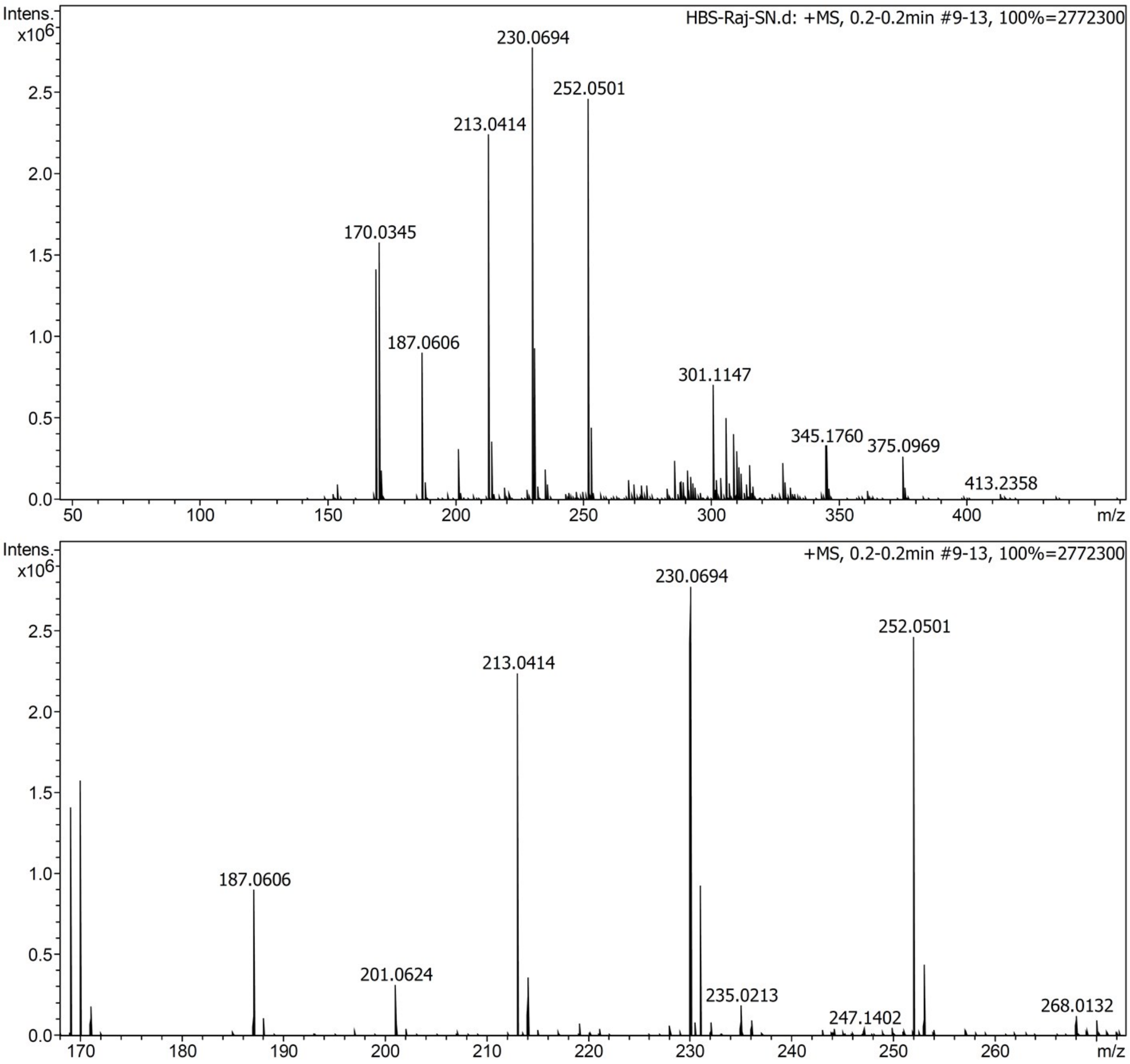

Figure S11: ES-MS spectra of **2-NOH-S**, m/z 230.06 calc. for (M+H+)

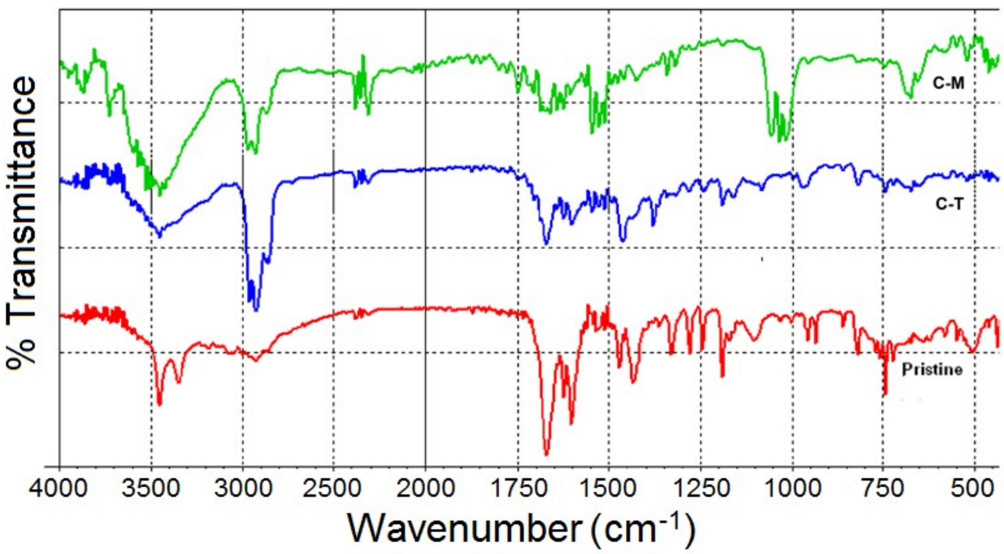

Figure S12: FTIR spectra of **C-M** and **C-T** forms, as compared to pristine sample of **2NOH-S**, depicting the variations in the absorptions due to the amide, imine and phenolic hydroxyl (recorded in the transmittance mode)

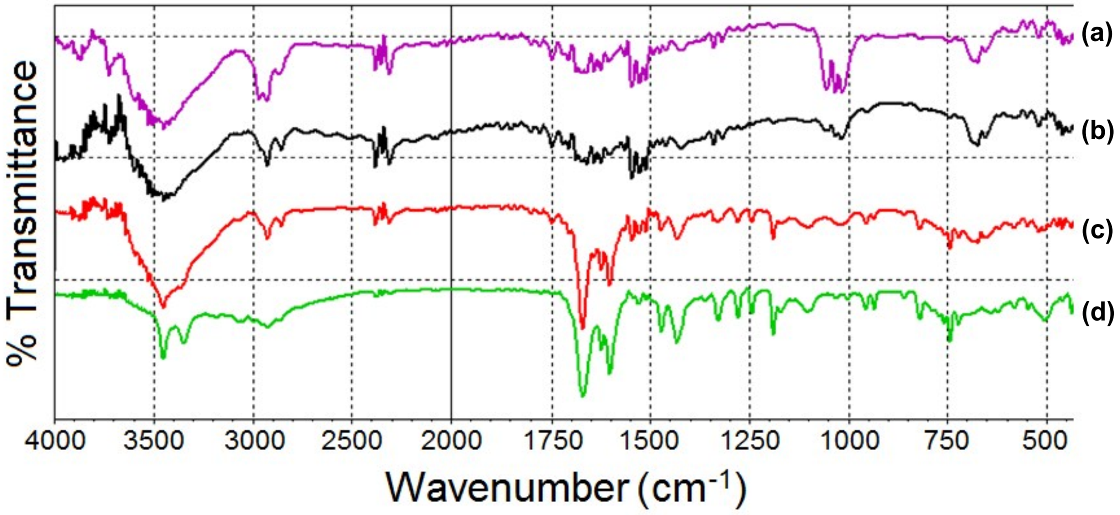

Figure S13: Variations observed in the FTIR spectra of **C-M** form after mechanical grinding, as function of grinding time

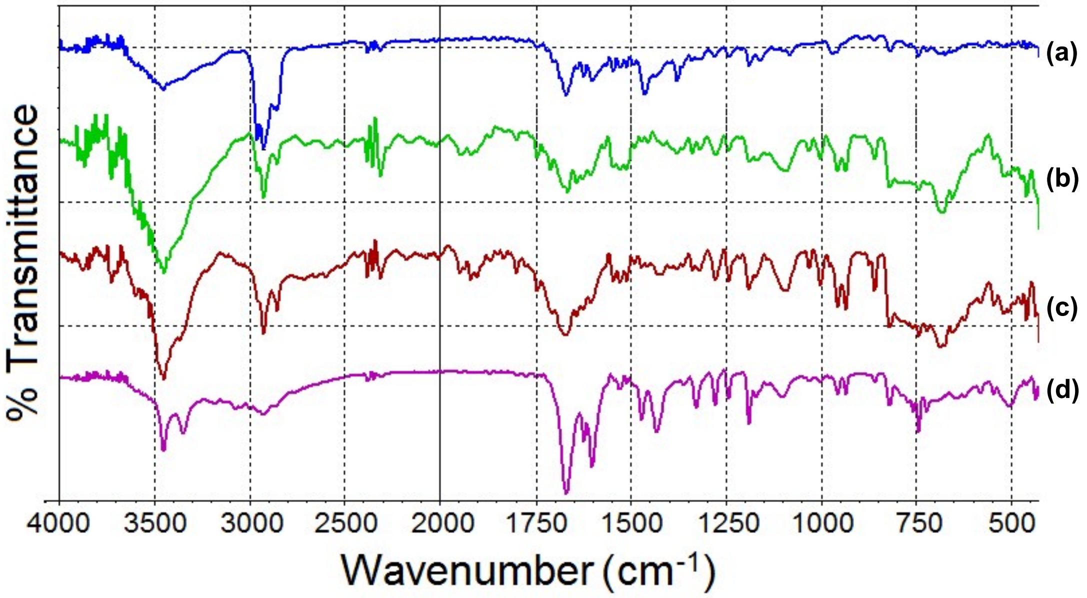

Figure S14: Changes in FTIR spectra of **C-T** upon mechanical stimulation; (a) **C-T** form, (b,c) after application of 0.9 MP and 3.0 MP pressure, as compared to (d) the pristine **2-NOH-S** sample.

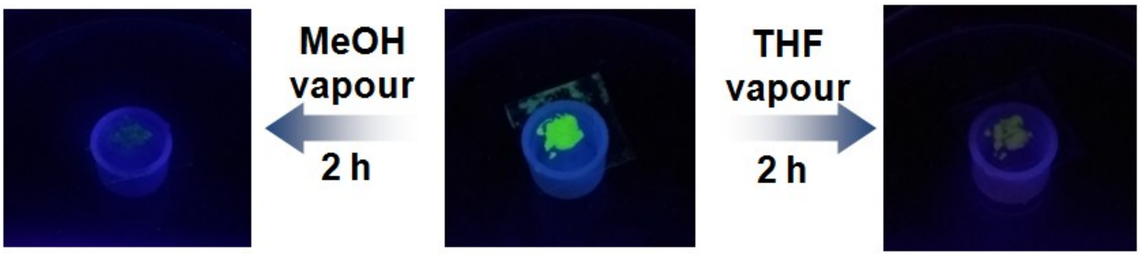

Figure S15: Effect of solvent vapour (methanol and tetrahydrofuran) on the mechano-luminescent emissions of the pristine form **2-NOH-S**. In a typical experiment, the mechano-luminescent phase was put on a glass slide, and kept in a closed petridish previously saturated with 3 mL of the solvent (covered with a petridish).

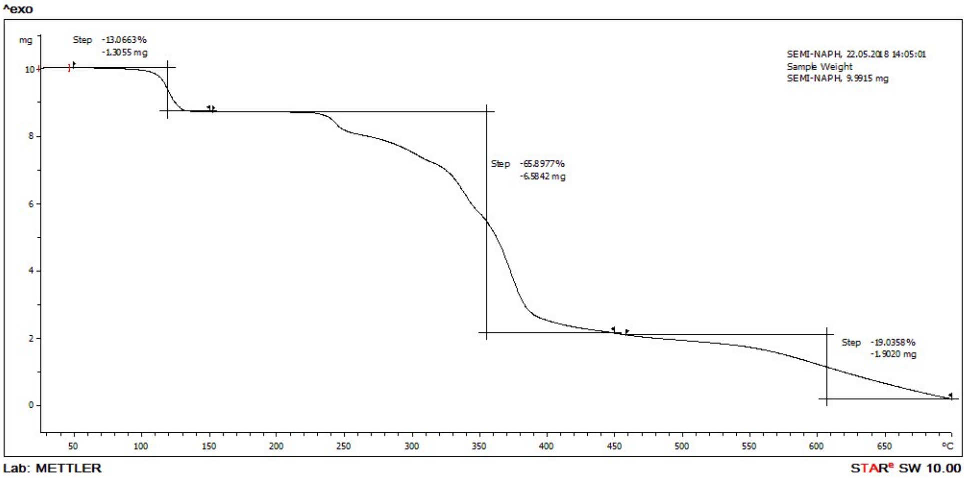

Figure S16: Thermo-gravimetric analysis (TGA) of **C-M** showing the weight loss corresponding to the removal of methanol from the sample.

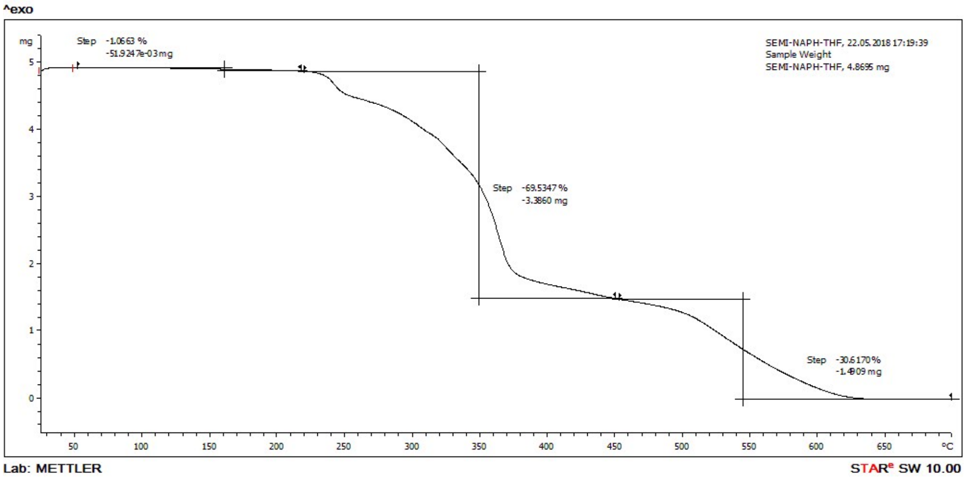

Figure S17: Thermo-gravimetric analysis (TGA) of **C-T**, which shows partial decomposition of the sample beyond approx. 250°C.

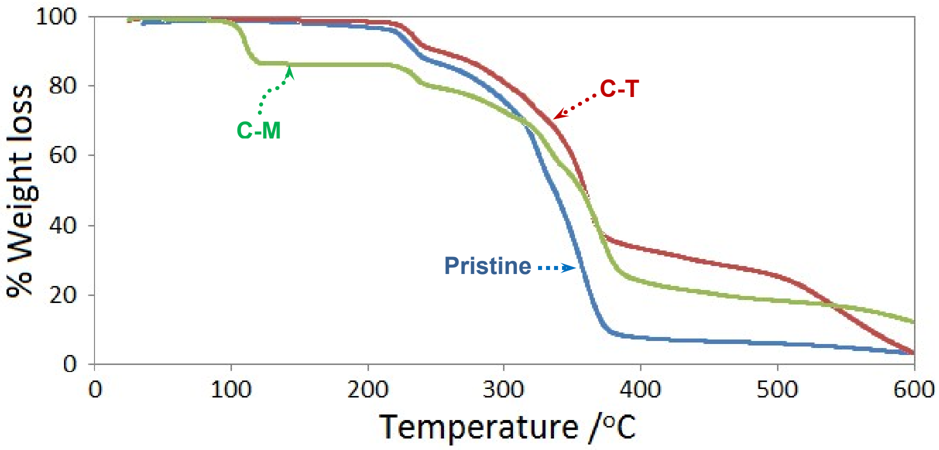

Figure S18: Comparison of TGA curves of **C-M** and **C-T** forms with the pristine form of **2-NOH-S**.

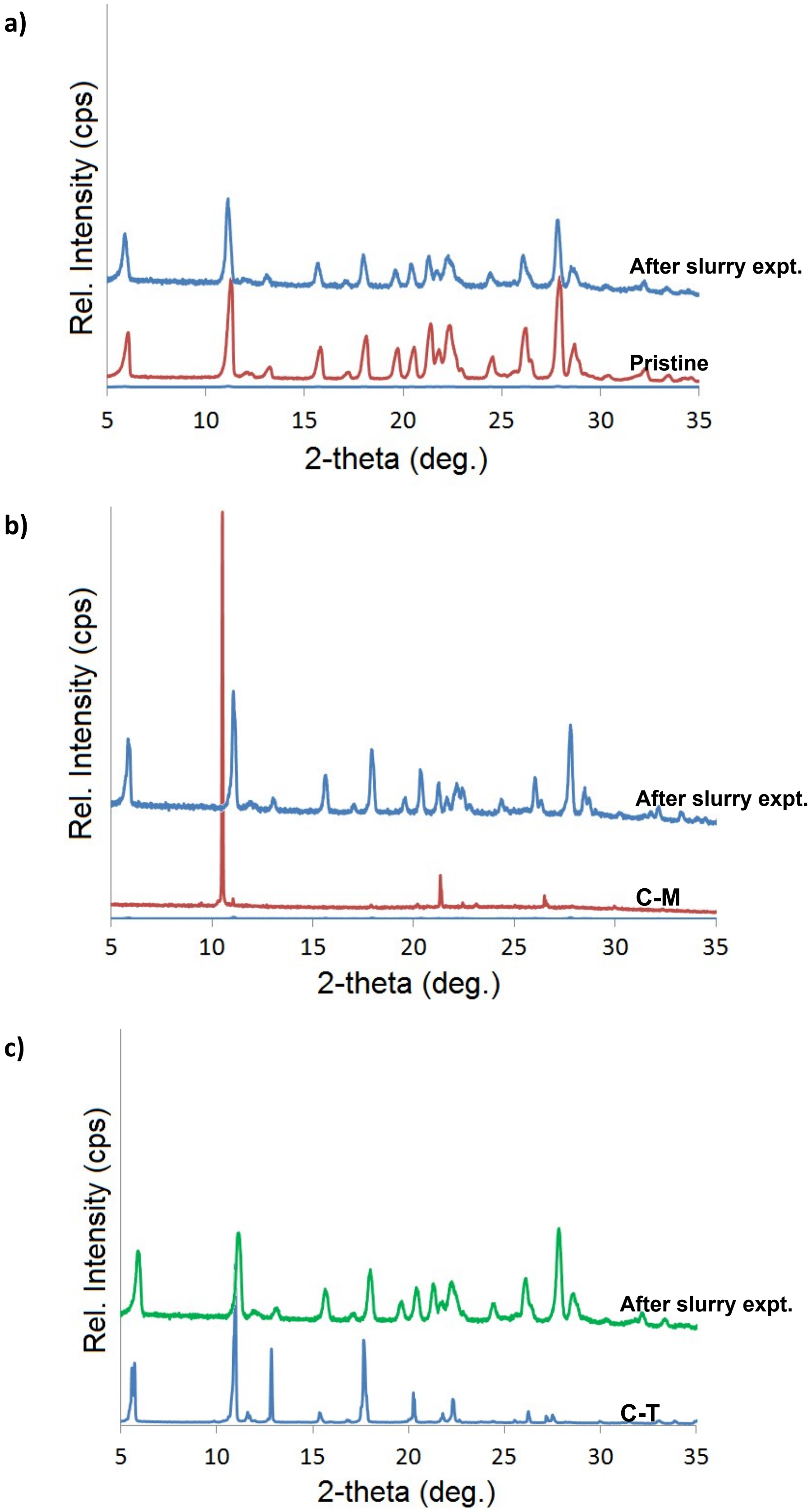

Figure S19: Representative powder XRD patterns obtained for the pristine form **C-M** and **C-T** when subjected to slurry experiments.

Table S1. Crystallographic parameters for **C-M** and **C-T** forms

Crystal	**C-M**	**C-T**
Empirical formula	$C_{12}H_{11}N_3O_2.CH_3OH$	$C_{12}H_{11}N_3O_2$
Formula weight	261.28	229.24
Temperature	296(2) K	296(2) K
Wavelength	0.71073 Å	0.71073 Å
Crystal system	Monoclinic	Monoclinic
Space group	$P\ 2_1/n$	$P\ 2_1/c$
Unit cell dimensions	a = 10.2378(11) Å, α = 90° b = 10.1117(9) Å, β = 92.895(5)° c = 13.0302(10) Å, γ = 90°	a = 16.1385(17) Å, α = 90° b = 4.7309(5) Å, β = 114.296(5)° c = 15.7978(17) Å, γ = 90°
Volume	1347.2(2) Å^3	1099.3(2) Å^3
Z	4	4
Density (calculated)	1.288	1.385
Absorption coefficient	0.094	0.098
F(000)	552	480
Theta range for data collection	3.131 to 26.393°	1.384 to 29.100°
Index ranges	-12<=h<=6, -12<=k<=12, -16<=l<=16	-21<=h<=22, -6<=k<=6, -21<=l<=19
Reflections collected	11012	10447
Independent reflections	2740	2915
Completeness to theta = 25.242°	99.6%	98.6%
Refinement method	Full-matrix least-squares on F^2	Full-matrix least-squares on F^2
Data / restraints / parameters	2740/0/193	2915/0/171
Goodness-of-fit on F^2	1.127	1.125
Final R indices [I>2sigma(I)]	R1 = 0.0436, wR2 = 0.0588	R1 = 0. 0602, wR2 = 0.0893
R indices (all data)	R1 = 0.1258, wR2 = 0.1450	R1 = 0.1476, wR2 = 0.1743
Largest diff. peak and hole	0.19, -0.26 Å^3	0.45, --0.36 Å^3